A Reliable Accelerated Protection Scheme for Converter-Dominated Power Networks

Subhadeep Paladhi, *Member, IEEE*, Qiteng Hong, *Senior Member, IEEE*, and Campbell Booth

***Abstract*—Rising penetration of converter-based sources with different control operations is introducing severe non-homogeneity in the power systems, especially during faults. Such non-homogeneity leads the decision derived by available distance and directional relays to be unreliable. Performances of the available communication-assisted tripping schemes being dependent on these two relay decisions at both ends become a concern for the protection of converter-dominated power networks. This work demonstrates the impact of converter-based sources on both distance and directional relays and the possible maloperation of the accelerated protection schemes. A new transfer trip scheme has been proposed mitigating the issue. Considering the homogeneity present in the negative and zero sequence networks in high voltage transmission system even with converter-based sources, two indices are derived using local voltage and current data to identify the fault direction at each end of a protected line. The decisions are transferred to the alternative ends through low-bandwidth communication channels to ensure the protection decision derived for the line to be dependable as well as secured. The scheme is tested for a 9-bus and a 39-bus system, even with 100% converter-based sources using PSCAD/ EMTDC simulation platform and found to be reliable for different faults and system conditions. Comparative assessment with a few advanced techniques demonstrates the superiority of the proposed method.**

***Index Terms*—Accelerated protection, transfer trip scheme, distance relaying, directional relaying, power system faults, Converter-interfaced renewable sources.**

I. Introduction

A. Motivation and Incitement

AMBITIOUS decarbonization target are enforcing power grids for large-scale integration of renewable energy sources [1], [2]. Integration of such sources necessitates numerous control functions to be employed in the interfacing converters to ensure reliable power system operation [3]. Converters controlled with grid-forming techniques are increasing to maintain stable grid operation with high renewable penetration [3], [4]. Different grid code requirements also enforce the control operations to adjust accordingly [5]. Diversity in control schemes compels converter-interfaced renewable energy sources (CIRES) to respond differently compared to conventional synchronous generators during fault. This modulates source impedances differently and results in a non-homogeneous situation in the grid [6]. Generation variability and intermittency associated with renewable sources intensify such complexity by varying the source-impedance-ratio (SIR) dynamically [7]. Such situations impel to revisit the performance of available protections schemes for the power networks dominated by converter-based sources. This article is an improved and expanded version of the paper presented at the 2022 22nd National Power Systems Conference [1].

B. Literature Review

With such variable SIR situations and increasing non-homogeneity in power systems, available local data-based protection schemes fail to derive correct decisions at times [6], [8], [9]. Line differential scheme employing both end current data communicated through dedicated communication channels are recommended for such a situation [10]. Cost associated with the required high-bandwidth dedicated communication channels and the communication latency are two major concerns for the wide-application of such a scheme for protection of transmission networks. Limited performance of current differential relays in renewable-connected lines also discourages for such a high investment [11]. Therefore, the transfer trip schemes requiring low-bandwidth communication channel are preferred [12]. Such schemes communicate the trip decision derived by local distance or directional units to the other end for ensuring secure and dependable accelerated protection for the lines. High and variable source impedance situations cause severe underreach and overreach issues with distance relays [13]. Different techniques are applied to enhance its performance in such situations, like multiple setting based approach [14]–[16], adaptive trip boundary setting [17], [18], application of data-driven techniques [19], [20], control-based adjustment [21], fault location mapping [8], and also by introducing intentional delay in decision [22]. Most of the techniques consider either the equivalent impedance associated with different sources to be negligible or the system to be homogeneous. The techniques applied for converter-based source connecting lines (like in [8]) are derived considering the grid connected at the remote end of the line to be strong and dominated by conventional synchronous generator based sources. None of these assumptions is true for converter-dominated power networks. Angular relation between voltage and current is also found to be inconsistent for faults in such a network resulting in maloperation of directional relays at times [9]. Such issues with the available distance and directional relaying impel to seek for a new technique to ensure correct performance of communication assisted tripping schemes for CIRES dominated power systems.

The work is supported in part by the Engineering and Physical Sciences Research Council (EPSRC), UK under Grant: EP/T021829/1 and IIT Indore, India under "Young Research Seed Grant Scheme (IITI/YFRSG/2023-24/Phase-III/05)".

Subhadeep Paladhi is with the Department of Electrical Engineering, Indian Institute of Technology Indore, India. (e-mail: spaladhi@iiti.ac.in)

Qiteng Hong and Campbell Booth are with the Department of Electronic & Electrical Engineering, University of Strathclyde, Glasgow, United Kingdom.

C. Contribution

In this work, the limited performance of available communication assisted tripping schemes are demonstrated for converter-dominated power systems and a novel scheme is proposed mitigating the issue. A new criteria is defined using local voltage and current data to identify the fault direction in power networks in the presence of converter-based sources. The proposed scheme uses a low-bandwidth dedicated communication channel to transfer decisions derived at both ends and issues a trip command when the fault is detected in forward direction at both ends of the line. The scheme is tested for a modified WSCC 9-bus system with 100% converter-based sources and a CIRES integrated 39-bus system using PSCAD/ EMTDC simulation data. The method is found to be accurate and independent of fault resistances, fault locations and different control operations associated with converters-based sources.

II. Problem Statement

This section first presents an overview of the available communication assisted transfer trip schemes used for accelerated protection of transmission networks and later demonstrates the limited performance of those schemes for a converter-dominated power system. Fig. 1(a) represents a two-bus equivalent power network, where the tripping zones for each end distance relay are shown in Fig. 1(b). The operating principle of four commonly used tripping schemes are described below.

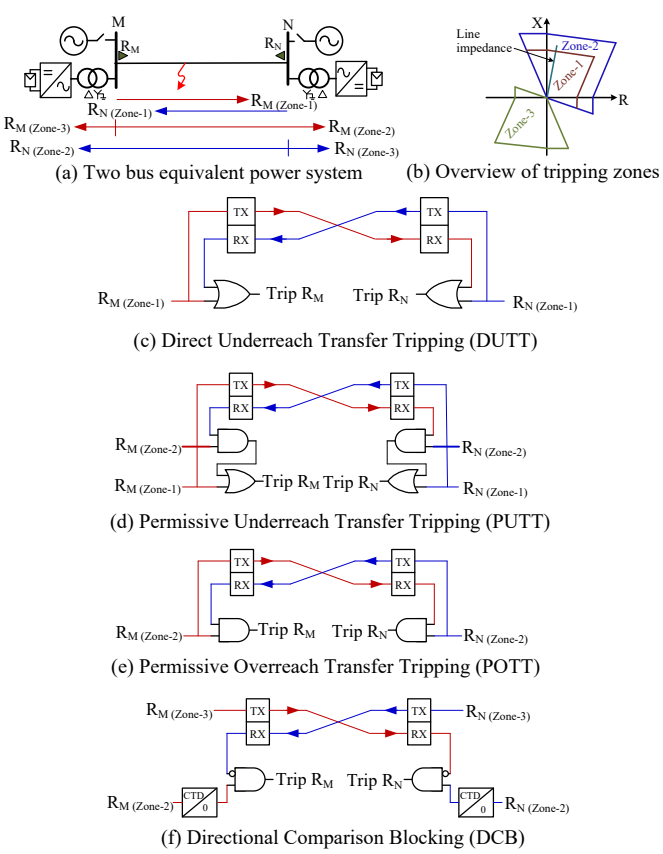

(a) Two bus equivalent power system (b) Overview of tripping zones

(c) Direct Underreach Transfer Tripping (DUTT)

(d) Permissive Underreach Transfer Tripping (PUTT)

(e) Permissive Overreach Transfer Tripping (POTT)

(f) Directional Comparison Blocking (DCB)

Fig. 1. Overview of common communication assisted transfer trip schemes.

- *Direct Underreach Transfer Tripping (DUTT)*: DUTT scheme, as shown in Fig. 1(c) issues a trip signal for both end circuit breakers when the fault is detected in Zone-1 by any of the relays (R_M and R_N) [12].
- *Permissive Underreach Transfer Tripping (PUTT)*: PUTT scheme employs Zone-1 decision at any end to trip the local breaker immediately and sends the decision to remote end as a permissive trip command. The permissive signal confirm the tripping of remote end breaker only when the corresponding relay finds the fault in Zone-2 using local data, as shown in Fig. 1(d) [12].
- *Permissive Overreach Transfer Tripping (POTT)*: POTT scheme (shown in Fig. 1(e)) issues a trip signal for both end circuit breakers when the fault is detected in Zone-2 by both end relays [12].
- *Directional Comparison Blocking (DCB)*: In this scheme, a trip command is generated when the fault is detected in Zone-2 by the local end relay and the remote end relay detects the fault outside of zone-3, as shown in Fig. 1(f) [12].

Now, the performances of the above mentioned schemes are tested for a 230 kV, 60 Hz modified WSCC 9-bus system with 100% converter-based sources, as shown in Fig. 2 [23], using PSCAD/ EMTDC simulation platform. The solar plant connected at bus $2'$ is integrated to the grid through grid-following converter, whereas the solar plants at bus 1 and 3 are integrated through grid-forming converters. The grid-following converter is controlled with balanced current controller, whereas the grid-forming converters are designed with dual-current controller mimicking synchronous generator negative sequence impedance angle characteristics [24]. Line 2-7 is considered here as the protected line and the performance of relay R_2 and R_7 are tested for the purpose with both distance and directional relaying principles, applying one at a time. Distance relays are set with quadrilateral characteristics as in [25] with a fault resistance coverage of 60Ω.

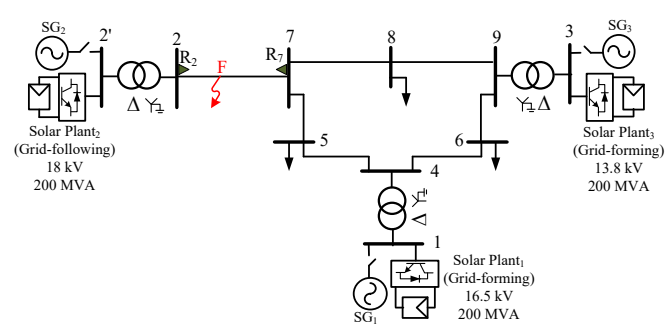

Fig. 2. Modified WSCC 9-bus system with 100% CIRESs.

A phase-B-to-phase-C-to-ground (BCG) fault is created in line 2-7 at a distance of $0.25\ pu$ from bus 2 with $R_F = 20\ \Omega$. Performance of the relays at bus 2 and bus 7 (R_2 and R_7), when incorporated with distance relaying principle, are demonstrated in Fig. 3. Results show that both the relays fail to identify the fault in corresponding Zone-1, which indicates a clear maloperation for DUTT and PUTT schemes. It is also observed that the relay R_2 finds the fault even outside its Zone-

2 boundary. This causes incorrect operation even when the PUTT and DCB schemes are applied. Such maloperation of distance relay is due to the non-homogeneity present between the fault currents fed through both ends of the faulted line. In this case, fault current at bus 2 is fed from the solar plant (connected at bus 2′) interfaced through grid-following converter, whereas the fault current at bus 7 is fed from two solar plants (connected at bus 1 and 3) interfaced through grid-following converters. Similar maloperation may also be experienced for faults in any other lines in the system.

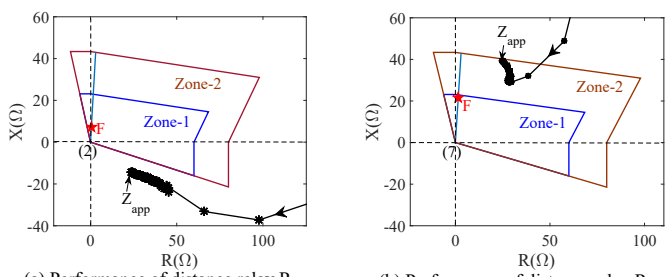

(a) Performance of distance relay R_2 (b) Performance of distance relay R_7

Fig. 3. Performance of both end distance relays leading to failure of available accelerated protection schemes.

The decisions derived using distance relay Zone-2 setting can also be derived using directional relaying principles [12]. Therefore, the performance of relay R_2 and R_7 are tested after employing superimposed component based directional relaying principle, which is applicable for all types of faults [26]. Results are provided in Fig. 4. ΔV_1 and ΔI_1 represent the positive sequence superimposed voltage and current components, which are obtained by subtracting 2-cycle memorized prefault data from the fault data [27]. According to the principle, the relay identifies the fault in forward direction when ΔV_1 lags ΔI_1 i.e. the angle difference between ΔV_1 and ΔI_1 is negative. Results in Fig. 4 show that the relay R_7 finds the fault in forward direction correctly, whereas the relay R_2 detects the fault in reverse direction. This results in maloperation of PUTT, POTT and DCB schemes, even when the directional principle is applied for the relays. Thus, there is a need for a new scheme for reliable protection of transmission lines in converter-based source dominated power systems.

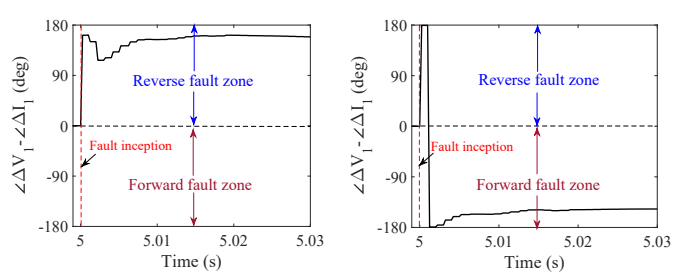

(a) Performance of directional relay R_2 (b) Performance of directional relay R_7

Fig. 4. Performance of both end directional relays leading to failure of available accelerated protection schemes.

III. Proposed Method

This section proposes a new technique for reliable and accelerated protection of converter-dominated power networks.

For the two-bus equivalent system in Fig. 1(a), apparent impedance (Z_{app}) calculated by the distance relay $\mathrm{R_M}$ for an AG fault, created at a distance of x pu from bus M and with a fault resistance $\mathrm{R_F}$, is given by [28],

$$Z_{app} = \frac{V_{AM}}{I_{AM} + K_0 I_{0M}} = xZ_{1L} + \left(\frac{I_{AF}}{I_{AM} + K_0 I_{0M}}\right) R_F. \quad (1)$$

Where, V_A and I_A are the voltage and current measurements respectively. 'M' in subscript represents the measurement at bus M and 'F' represents the the variables in the faulted path. $\mathrm{Z_L}$ represents the impedance of line MN. Subscript '0' and '1' indicate the zero and positive sequence components respectively. K_0 is the zero sequence compensation factor. Fig. 5 represents the sequence network of the system in Fig. 1(a) for AG faults. 'RN' in subscript represents the equivalent representation of the renewable sources connected to the bus, whereas 'S' indicates the conventional sources which are considered here to be out of operation. '2' in the position of first subscript indicates negative sequence components. M end is considered to be connected to a renewable source through a grid-following converter. Therefore, the positive sequence source-equivalent of this side is represented by a dependent current source in parallel with a variable impedance [8]. The converter is considered to be controlled with balanced current controller. So it cannot inject negative sequence current even during asymmetrical faults. On the other hand, the N end is considered to be connected to a renewable source through grid-forming converter and controlled using dual-current controller mimicking synchronous generator negative sequence impedance angle characteristics. Positive and negative sequence source-equivalents are represented with a dependent voltage source with a variable series impedance. A dependent voltage source can also be transformed to an equivalent current source at each instant [6]. Therefore, the sequence network presented in Fig. 5 is a generalized representation for a converter dominated power network.

I_{1F}, I_{2F} and I_{0F} being equal, I_{AF} in (1) can be replaced by I_{0F}, as in (2).

$$\frac{V_{AM}}{I_{AM} + K_0 I_{0M}} = xZ_{1L} + \left(\frac{3I_{0F}}{I_{AM} + K_0 I_{0M}}\right) R_F. \quad (2)$$

(2) is rewritten in (3) by expanding the variables with their complex forms.

$$\frac{|V_{AM}|}{|I_{AM}+K_0 I_{0M}|} e^{j(\alpha-\beta)} = x|Z_{1L}|e^{j\theta_{1L}} + \frac{|3I_{0F}|}{|I_{AM}+K_0 I_{0M}|} e^{j(\gamma-\beta)} R_F \quad (3)$$

α and β are the phase angles of V_{AM} and $(I_{AM} + K_0 I_{0M})$. θ_{1L} and γ represent the line impedance angle and the phase angle of I_{0F} respectively. (3) is rewritten in (4).

$$\frac{|V_{AM}|}{|I_{AM}+K_0 I_{0M}|} e^{j(\alpha-\gamma)} = x|Z_{1L}|e^{j(\theta_{1L}-\gamma+\beta)} + \frac{|3I_{0F}|}{|I_{AM}+K_0 I_{0M}|} R_F \quad (4)$$

(5) is derived by comparing the imaginary parts of both sides in (4).

$$\frac{|V_{AM}|}{|I_{AM} + K_0 I_{0M}|} \sin(\alpha - \gamma) = x|Z_{1L}| \sin(\theta_{1L} - \gamma + \beta) \quad (5)$$

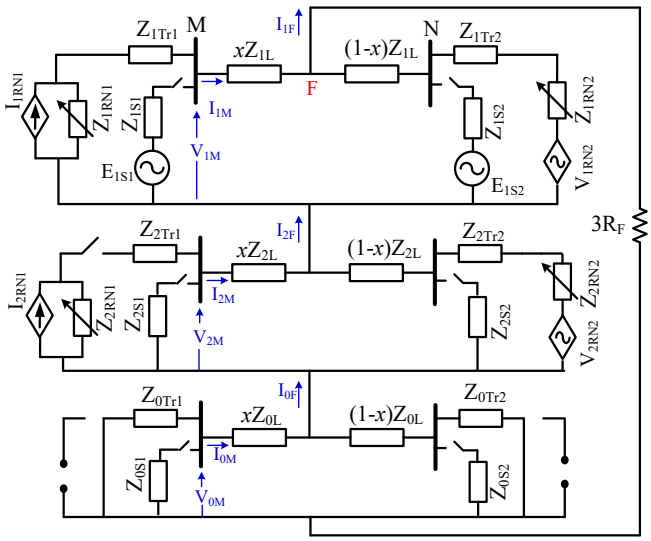

Fig. 5. Sequence networks of the system in Fig. 1(a) for AG faults.

From (5), x can be computed as in (6).

$$x = \frac{S_{1M}}{S_{2M}} \tag{6}$$

Where,

$$S_{1M} = \frac{|V_{AM}|}{|I_{AM} + K_0 I_{0M}|} \sin(\alpha - \gamma)$$
$$S_{2M} = |Z_{1L}| \sin(\theta_{1L} - \gamma + \beta).$$

Renewable sources at both ends are connected to the grid through a dYg-type transformer. Therefore, the zero sequence network remain homogeneous as considered for a system without renewable sources. Thus, γ is the angle of zero sequence current measured at bus M. For other types of faults, S_{1M} and S_{2M} used in the new directional criteria proposed in (8) are derived in Appendix. For all types of faults, S_{1M} and S_{2M} are expressed in a generalized form in (7).

$$S_{1M} = \frac{|V_{RM}|}{|I_{RM}|} \sin(\alpha - \gamma)$$
$$S_{2M} = |Z_{1L}| \sin(\theta_{1L} - \gamma + \beta). \tag{7}$$

where V_{RM} and I_{RM} are the operating voltage and current for the relay at bus M.

x is always positive for any fault in the forward direction. Thus, a new directional criteria for converter-dominated power network is proposed in (8).

$$\frac{S_{1M}}{S_{2M}} = \begin{cases} > 0; & for\ forward\ fault \\ < 0; & for\ reverse\ fault \end{cases} \tag{8}$$

Using this criteria, a transfer trip scheme is proposed. The scheme issues trip command only when the fault is identified in forward direction at both ends, which is similar to POTT [12] but applies the proposed directional criteria for deriving the decisions. Steps associated with the proposed scheme are shown in Fig. 6. Currents and voltages at each end are obtained from local current transformer (CT) and capacitor voltage transformer (CVT) respectively. A combination of undervoltage and overcurrent principle is applied for fault detection. A zero sequence overcurrent check is also used in parallel to enhance the fault detection sensitivity for ground faults with high R_F. A local voltage based techniques, as available in [29], is applied for fault classification.

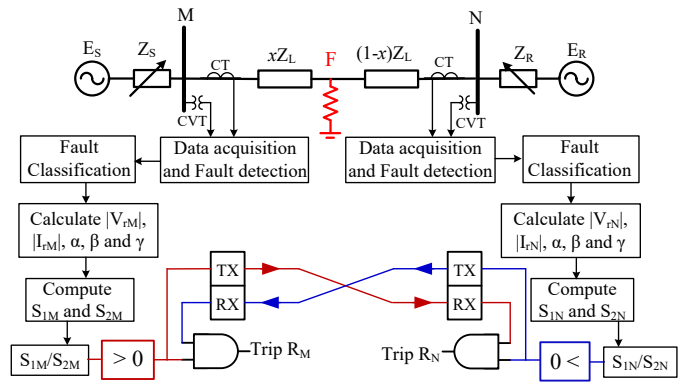

Fig. 6. Proposed transfer trip scheme logic implementation.

IV. Results

Performance of the proposed protection scheme is tested in the 9-bus system of Fig. 2 with 100% converter-based sources and a CIRES-integrated 39-bus system, as shown in Fig. 7 using PSCAD/ EMTDC simulation platform for different faults with variation in some critical parameters. Solar and wind farms integrated to the 39-bus system are of 300 MVA each with the specifications as provided in [30] and controlled with balanced current controller. Type-III and Type-IV wind farm are complied with standard control schemes as available in [31], [32]. Voltage and current phasors are estimated using 1-cycle discrete Fourier transform at a sampling rate of 64 samples/ cycle.

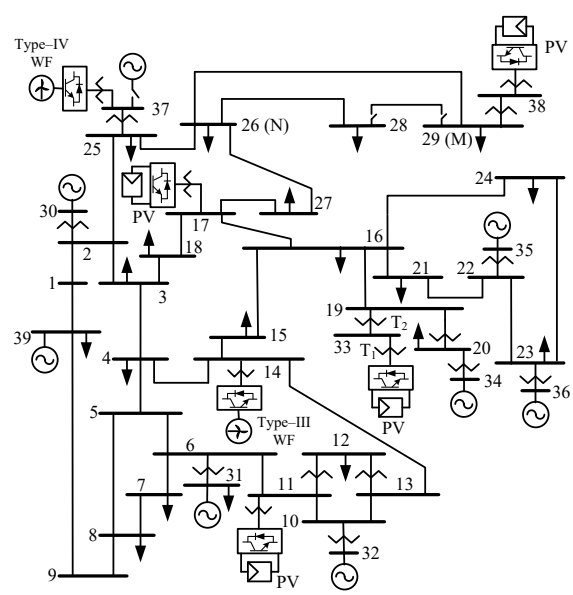

Fig. 7. Converter-based source integrated 39-bus system.

A. Performance evaluation in a 9-bus system system with 100% converter-based sources

Performance of the proposed method is tested for two faults (internal and external with respect to the line 2-7 of the system in Fig. 2). The first case is same as mentioned in Section II i.e for a BCG fault created in line 2-7 at a distance of $0.25\ pu$ from bus 2 with $R_F = 20\ \Omega$. It has already been demonstrated that all the communication assisted trip schemes fail to protect the line correctly when both end relays are incorporated with conventional distance or directional relaying principles. Results in Fig. 8 show that relays at both ends of line 2-7 calculates the directional index as proposed in this work are positive (0.24 and 0.73). Thus, the method identifies the internal fault correctly satisfying the conditions in (8) and issues trip command for both end circuit breakers.

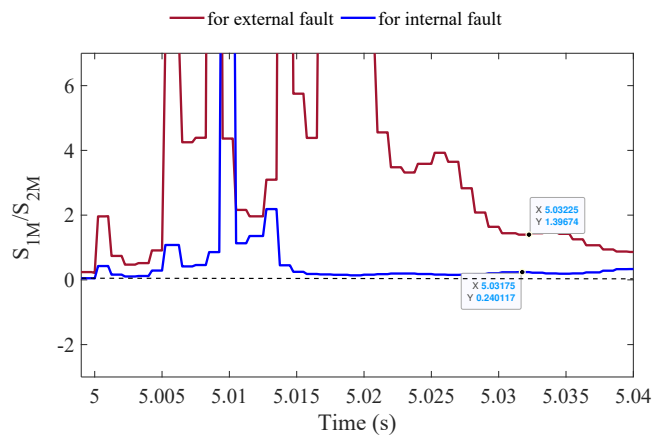

(a)

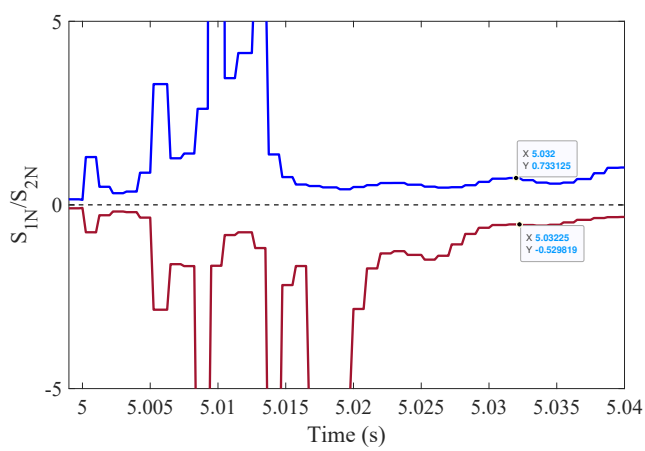

(b)

Fig. 8. Performance of (a) R_2 and (b) R_7 with the proposed method for a system with 100% CIRESs.

In the second case, a BCG fault is created in line 7-8 of the system in Fig. 2 at a distance of $0.5\ pu$ from bus 7 with $R_F = 15\ \Omega$. From the results in Fig. 8, it is observed that the relay at bus 2 calculates the directional index as positive (=1.40) using the proposed method, whereas the relay at bus 7 calculates it as negative (=-0.53). Thus, the proposed scheme maintains security correctly even for external fault.

B. For different faults created at different locations with variation in $\mathrm{R_F}$

Performance of the proposed method is now tested for different faults created in the CIRES-integrated 39-bus test system, as shown in Fig. 7 varying the fault location (x) and associated fault resistance ($\mathrm{R_F}$). $\mathrm{R_F}$ for ground faults is varied up to 100 Ω. Line 28-29 is considered to be out-of-operation for this study and the performances of relays at both ends of line 29-26 are tested incorporating the proposed protection technique. Results obtained for different cases are provided in Table I. It is observed that both relays at bus 29 and bus 26 calculate the directional index as positive when the fault created at any location in line 29-26 and derive the decision for all internal faults correctly. For faults created in line 25-26, relay at bus 29 calculates the index as positive and confirm the fault to be in forward direction, whereas relay at bus 26 calculates the index as negative for all the cases and maintains security for such external faults. Results validate the method to be applicable for all types of faults and also to be independent of fault locations and fault resistances.

TABLE I
DIRECTIONAL INDICES CALCULATED AT BOTH LINE ENDS FOR DIFFERENT FAULTS WITH VARIATION IN ASSOCIATED PARAMETERS

Fault Type	$\mathrm{R_F}$ (Ω)	$x = 0.1pu$ from (29)		$x = 0.5pu$ from (29)		$x = 0.9pu$ from (29)		Faults in line 25-26	
		$\mathrm{R_{29}}$	$\mathrm{R_{26}}$	$\mathrm{R_{29}}$	$\mathrm{R_{26}}$	$\mathrm{R_{29}}$	$\mathrm{R_{26}}$	$\mathrm{R_{29}}$	$\mathrm{R_{26}}$
AG	1	0.09	0.88	0.52	0.51	0.91	0.09	1.28	-0.33
	10	0.11	0.89	0.51	0.49	0.88	0.10	1.33	-0.31
	100	0.13	0.93	0.47	0.48	0.85	0.12	1.37	-0.27
BC	0.5	0.08	0.89	0.48	0.49	0.90	0.09	1.29	-0.32
	30	0.11	0.94	0.52	0.47	0.93	0.08	1.34	-0.27
BCG	1	0.08	0.89	0.48	0.51	0.91	0.11	1.29	-0.32
	10	0.09	0.90	0.49	0.50	0.90	0.11	1.31	-0.29
	100	0.13	0.95	0.46	0.48	0.86	0.08	1.37	-0.24
ABC	0.5	0.12	0.90	0.47	0.51	0.92	0.11	1.29	-0.33

C. For generation variation in the renewable plant connected to the protected line

Variation in renewable plant generation influences the equivalent source impedance significantly. Such a situation degrades the performance of protective relays. Therefore, it is necessary to evaluate the performance of the proposed protection technique under similar situations. For this purpose, BCG faults are created in line 29-26 of the system in Fig. 7 at a distance of $0.4\ pu$ from bus 29 with $\mathrm{R_F} = 30\Omega$, while the generation of the solar plant connected at bus 29 is varied from 25% to 100%. Line 28-29 is considered to be out-of-operation. Similar values for S_1 and S_2 calculated by the relays at bus 29 and bus 26 for all the cases (as shown in Fig. 9(a)) demonstrate these variables to be adaptive to the generation variation of the renewable plant. Results shown in Fig. 9(b) verify that the generation variation cannot affect the directional index proposed in this work. Positive and consistent values of the indices confirm correct operation of the proposed method for all the cases with variation in CIRES generation.

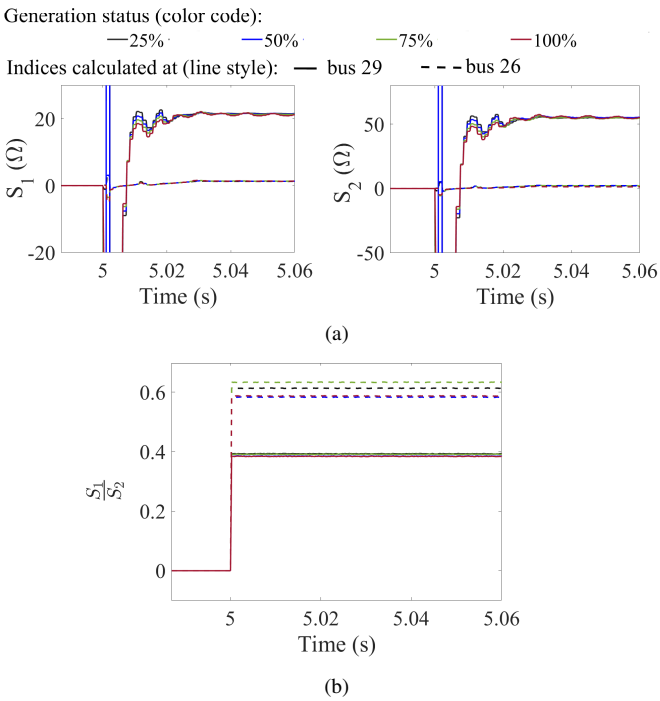

Fig. 9. Performance of the proposed method with variation in generation of CIRES connected to the line.

D. With CIRESs satisfying different grid code requirements

CIRESs need to satisfy the grid code requirements to remain connected to the grid, especially during faults. Variation in grid code influences the converter-control operation to act accordingly, especially the reactive current injection for supporting the low voltage situations. For an example, the German grid code introduces a proportionality constant (k) to determine the required reactive current in relation to the voltage deviation. k varies in the range of $0-10$ based on the agreement with network operators, with a default value of 2. Variation of reactive current (I_q) generation with respect to the voltage drop ($\frac{\Delta V}{V_n}$) during fault for four different European grid codes are shown in Fig. 10 [33]. Here, I_n and V_n are the nominal current and voltage respectively. Such variation in I_q modulates the phase angle associated with fault current significantly, and affects relay operations at times. Performance of the proposed protection scheme is tested for AG faults created in line 29-26 at a distance of 0.6 pu from bus 29 with $\mathrm{R_F} = 35\Omega$, when the converter interfacing the solar plant connected to bus 29 is controlled to satisfy North American grid-code (NAGC) and European Union grid code (EUGC), one at a time. The converter operates within a power factor range of 0.95 lag to 0.95 lead while complied with NAGC, whereas it prioritizes reactive current generation when complied with EUGC [5], [21]. Results in Fig. 11(a) show the variation in S_1 and S_2 computed by the relays at bus 29 and bus 26 with the change in grid code requirements as imposed on the connected CIRES interfacing converter. Such variations in S_1 and S_2 cannot affect the directional index proposed in this work. From the results shown in Fig. 11(b), it is observed that the index computed for both the situations are almost same and positive. Thus, the proposed scheme performs accurately even with the variation in grid code requirements imposed for the converter-control operation.

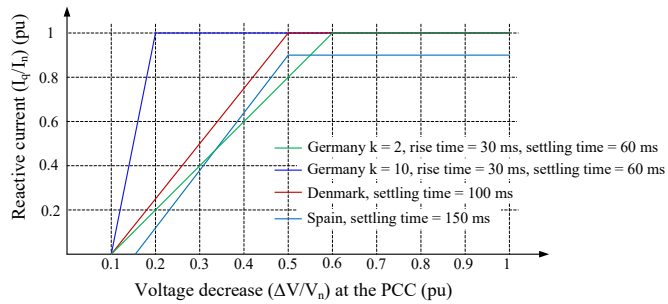

Fig. 10. Reactive current requirement with voltage dip for different grid codes.

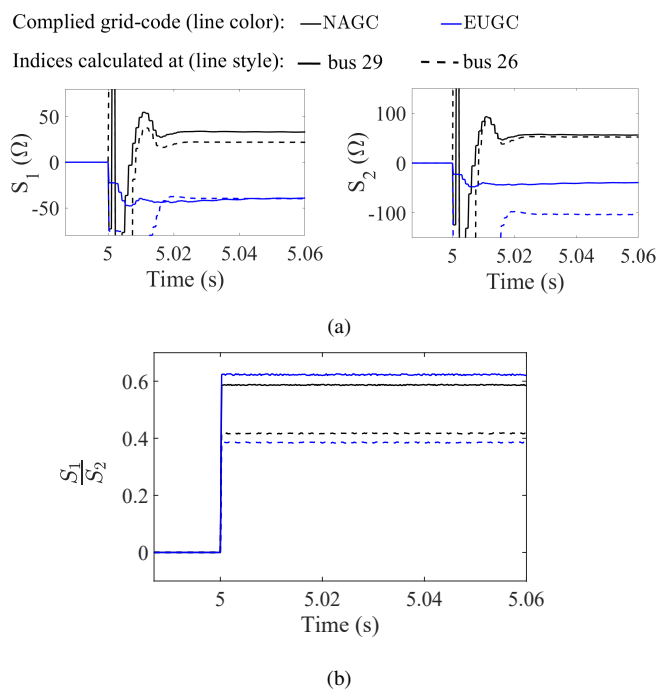

Fig. 11. Performance of the proposed method with CIRESs complied with different grid code requirements.

E. In the presence of different CIRESs connected to the protected line

Different types of CIRESs are integrated to the grid with different converter arrangements modulating the voltage and current signals differently during faults. This may affect relay operations significantly. Performance of the proposed method is tested for such a situation, when BCG faults are created in line 29-26 at a distance of 0.4 pu from bus 29 with $\mathrm{R_F} = 30\Omega$ and the solar plant connected to bus 29 is replaced by Type-III and Type-IV wind farms of same capacity, one at a time. Variations in S_1 and S_2 computed by the relays at both ends of the line 29-26 for all situations are shown in Fig. 12(a). The directional index ($\frac{S_1}{S_2}$) calculated at both ends, as shown in Fig. 12(b) are found to be consistent and positive for all the situations. Thus, the proposed method

derives protection decisions correctly satisfying the criteria in (8). This declares the method to be independent of the converter-control operation with different renewable sources.

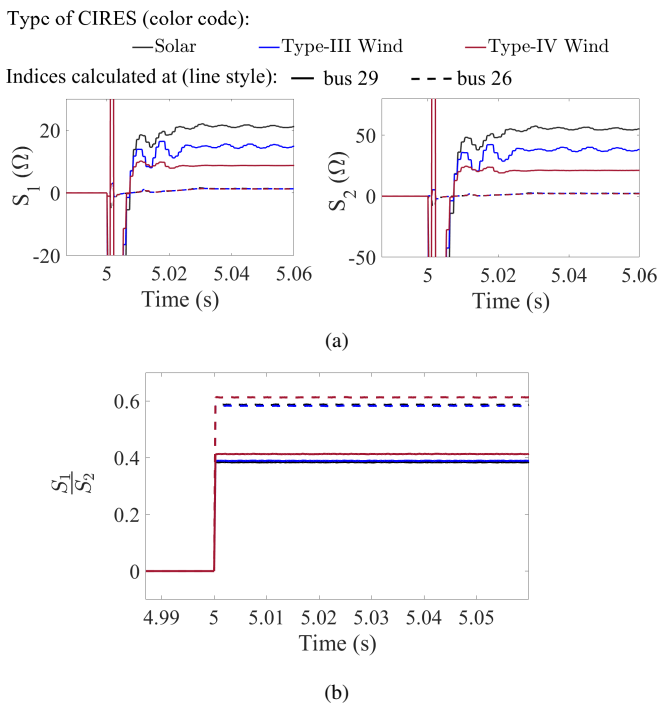

Fig. 12. Performance of the proposed method for different types of CIRESs connected to the line.

F. Comparative assessment

Different techniques are being tested to prevent the growing maloperation issues with conventional distance and directional relays in the presence of CIRESs. Features of the proposed method is now compared with some of those techniques, available in [8], [22], [34]–[36]. The comparative assessment in Table II clearly reveals the novelty and necessity of the proposed method for the present power systems moving towards decarbonization.

TABLE II
COMPARATIVE ANALYSIS WITH RECENT AVAILABLE METHODS

Parameters	Available Methods					Proposed Method
	[34]	[35]	[36]	[22]	[8]	
Applicable for all relays in the system?	No	No	No	No	No	Yes
Independent of converter-control operations?	Yes	No	No	Yes	Yes	Yes
Can perform for all types of faults?	No	Yes	No	Yes	Yes	Yes
Performs correctly in weak-grid condition?	Yes	No	Yes	No	No	Yes
Tested for systems with high renewable penetration?	No	No	No	No	No	Yes

V. CONCLUSION

Power grid is experiencing a noticeable change in fault characteristics with growing penetration of converter-based renewable sources. Conventional distance and directional relaying decisions derived in such a new grid scenario is found to be unreliable. This work demonstrates the impact of CIRESs on communication assisted accelerated protection schemes, where the trip decisions are generated and supervised by conventional distance and/ or directional relays. The work proposes a new criteria to identify the fault direction in converter-dominated power networks using local voltage and current data. The directional decisions derived at both ends are transferred mutually through a low-bandwidth dedicated communication channel to generate a secure and dependable trip command for the line end breakers. The method is derived using the homogeneity present in negative and zero sequence networks in high voltage transmission grids, even with CIRESs. This generalizes the method for application in any transmission network with or without CIRESs. The method is tested for a 9-bus system with 100% converter-based sources and a CIRES integrated 39-bus system. The method is found to be reliable for faults created at different locations, with different fault resistances, in the presence of CIRESs with different control operations satisfying grid code requirements. The proposed protection scheme addresses two important concerns for the present power systems. It performs correctly being independent of the behavior of the sources feeding the fault current. In addition, accelerated protection decisions from both ends help in reliable and quick isolation of the faulted part which helps in maintaining system stability in low-inertia situations as being experience with growing penetration of converter-based sources. Comparative assessment with a few advanced protection techniques reveals the novelty of the proposed method and justifies its requirement in the new power grid scenario. The work can be further extended for applying in low voltage distribution grids, where a significant non-homogeneity may present between negative and zero sequence networks.

APPENDIX

Sequence networks of the system in Fig. 1(a) for BCG, BC and 3-phase faults are shown in Fig. 13.

A. For BCG faults

Applying Kirchhoff's Voltage Law (KVL) in the faulted loop of the sequence network in Fig. 13(a) and rearranging the variables, Z_{app} calculated by the distance relay $\mathrm{R_M}$ for a BCG fault, created at a distance of x pu from bus M and with a fault resistance $\mathrm{R_F}$, can be expressed as,

$$\frac{V_{2M}-V_{0M}}{I_{2M}-K_0' I_{0M}} = xZ_{1L} - \frac{I_{0F}}{I_{2M}-K_{0L}' I_{0M}} \left((1-d)\, R_{ph} + 3R_F\right). \quad (9)$$

where, $K_{0L}' = \frac{Z_{0L}}{Z_{1L}}$ and $d = \frac{I_{2F}}{I_{0F}}$. Arcing resistance R_{ph} is negligible to $\mathrm{R_F}$ for high resistance faults. Homogeneity in the equivalent negative and zero sequence networks results in d to be a real term for solid faults with low $\mathrm{R_F}$. Comparing (9) with (2), S_{1M} and S_{2M} for BCG faults can be expressed as in (10).

$$\begin{aligned} S_{1M} &= \frac{|V_{2M}-V_{0M}|}{|I_{2M}-K_0' I_{0M}|} \sin(\alpha-\gamma) \\ S_{2M} &= |Z_{1L}| \sin(\theta_{1L} - \gamma + \beta). \end{aligned} \quad (10)$$

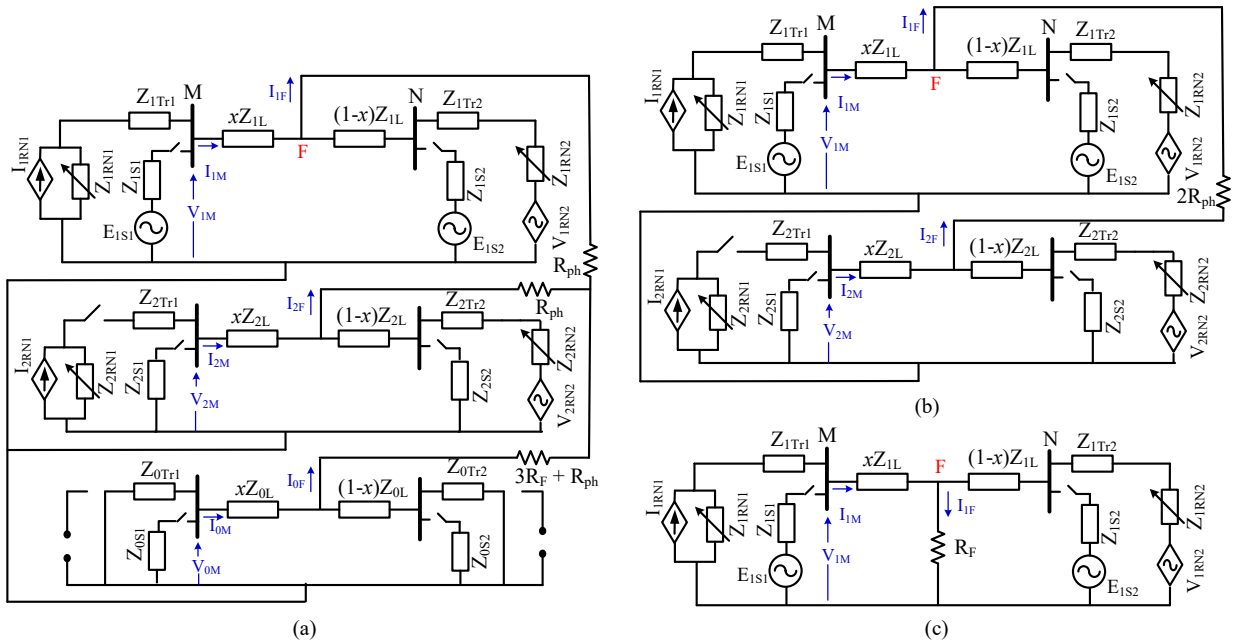

Fig. 13. Sequence networks of the system in Fig. 1(a) for (a) BCG, (b) BC and (c) 3-phase faults.

where,

$$\alpha = arg\left(V_{2M} - V_{0M}\right),\ \beta = arg\left(I_{2M} - K_0' I_{0M}\right),$$
$$\gamma = arg(-I_{0F}) = arg(I_{0M}) - \pi$$

B. For BC faults

Applying KVL in the faulted loop of the sequence network in Fig. 13(b) and rearranging the variables, Z_{app} calculated by the distance relay $\mathrm{R_M}$ for a BC fault, created at a distance of $x\ pu$ from bus M and with a fault resistance $\mathrm{R_F}$, can be expressed as,

$$\frac{V_{1M} - V_{2M}}{I_{1M} - I_{2M}} = xZ_{1L} - \frac{2I_{2F}}{I_{1M} - I_{2M}} R_{ph}. \tag{11}$$

Comparing (11) with (2), S_{1M} and S_{2M} for BC faults are expressed in (12).

$$\begin{aligned} S_{1M} &= \frac{|V_{1M} - V_{2M}|}{|I_{1M} - I_{2M}|} \sin\left(\alpha - \gamma\right) \\ S_{2M} &= |Z_{1L}| \sin\left(\theta_{1L} - \gamma + \beta\right). \end{aligned} \tag{12}$$

where,

$$\alpha = arg\left(V_{1M} - V_{2M}\right), \beta = arg\left(I_{1M} - I_{2M}\right), \gamma = arg(-I_{2F})$$

Bus M being connected to a grid-following converter-interfaced renewable plant controlled with balanced current controller, no negative sequence current is measured at M. CIRES connected at bus N being controlled with dual current controller mimicking synchronous generator's negative sequence impedance, Z_{2S2} can be expressed as, $Z_{2S2} = mZ_{2L}$, where m is a real-valued multiplier. For such a situation, I_{2F} can be obtained as in (13).

$$I_{2F} = -\frac{V_{2F}}{(1-x)Z_{2L} + Z_{2S2}} \approx -\frac{V_{2M}}{(1-x+m)Z_{2L}} \tag{13}$$

Thus, γ for BC fault is derived for relay $\mathrm{R_M}$ as follows.

$$\gamma = arg(-I_{2F}) = arg\left(\frac{V_{2M}}{Z_{2L}}\right) \tag{14}$$

On the other hand, I_{2F} flows only through the bus N. Therefore for relay $\mathrm{R_N}$, γ for BC fault is obtained as in (15).

$$\gamma = arg(-2I_{2F}) = arg(I_{2N}^{f}) - \pi \tag{15}$$

C. For 3-phase faults

Only positive sequence components are presents for 3-phase faults, as shown in Fig. 13(c). Z_{app} calculated by the distance relay $\mathrm{R_M}$ for a 3-phase fault, created at a distance of $x\ pu$ from bus M and with a fault resistance $\mathrm{R_F}$, can be expressed as,

$$\frac{V_{1M}}{I_{1M}} = xZ_{1L} + \frac{I_{1F}}{I_{1M}} R_F. \tag{16}$$

For 3-phase faults, $\mathrm{R_F}$ is considered to be very small ($< 1\Omega$) [37]. Thus, the value of $\frac{I_{1F}}{I_{1M}} R_F$ in (16) becomes negligible, especially when the imaginary parts of both sides are compared (as done in (5) for obtaining S_{1M} and S_{2M}). Therefore, (16) can be simplified as in (17).

$$\frac{V_{1M}}{I_{1M}} = xZ_{1L}. \tag{17}$$

Comparing (17) with (2), S_{1M} and S_{2M} for 3-phase faults can be expressed as in (18).

$$\begin{aligned} S_{1M} &= \frac{|V_{1M}|}{|I_{1M}|} \sin\left(\alpha - \beta\right) \\ S_{2M} &= |Z_{1L}| \sin\left(\theta_{1L}\right). \end{aligned} \tag{18}$$

where,

$$\alpha = arg\left(V_{1M}\right) \text{ and } \beta = arg\left(I_{1M}\right)$$

References

[1] S. Paladhi, Q. Hong, and C. Booth, "A reliable accelerated protection scheme for converter-dominated power networks," in *22nd National Power Systems Conference (NPSC)*, 2022, pp. 654–657.

[2] "Renewables integration in india," NITI Ayog, International Energy Agency, Tech. Rep., April 2021, [Online]. Available: https://iea.blob.core.windows.net/assets/7b6bf9e6-4d69-466c-8069-bdd26b3e9ed1/RenewablesIntegrationinIndia2021.pdf.

[3] ESIG, "Grid-forming technology in energy systems integration," Energy Systems Integration Group, Tech. Rep., March 2022.

[4] W. Du, F. K. Tuffner, K. P. Schneider, R. H. Lasseter, J. Xie, Z. Chen, and B. Bhattarai, "Modeling of grid-forming and grid-following inverters for dynamic simulation of large-scale distribution systems," *IEEE Transactions on Power Delivery*, vol. 36, no. 4, pp. 2035–2045, 2021.

[5] IRENA, "Grid codes for renewable powered systems," International Renewable Energy Agency, Abu Dhabi, Tech. Rep., April 2022.

[6] S. Paladhi and A. K. Pradhan, "Adaptive fault type classification for transmission network connecting converter-interfaced renewable plants," *IEEE Syst. J.*, vol. 15, no. 3, pp. 4025–4036, 2021.

[7] S. Paladhi, "Distance protection for lines connecting converter-interfaced renewable sources," Ph.D. dissertation, IIT Kharagpur, 2021.

[8] S. Paladhi and A. K. Pradhan, "Adaptive distance protection for lines connecting converter-interfaced renewable plants," *IEEE J. Emerg. and Sel. Topics Power Electron.*, vol. 9, no. 6, pp. 7088–7098, 2021.

[9] K. Jia, Z. Yang, Y. Fang, T. Bi, and M. Sumner, "Influence of inverter-interfaced renewable energy generators on directional relay and an improved scheme," *IEEE Trans. Power Electr.*, vol. 34, no. 12, pp. 11 843–11 855, Dec 2019.

[10] Y. Xue, B. Kasztenny, D. Taylor, and Y. Xia, "Series compensation, power swings, and inverter-based sources and their impact on line current differential protection," in *Proc. 66th Annual Conf. Prot. Relay Engineers*, April 2013, pp. 80–91.

[11] A. Chowdhury, S. Paladhi, and A. K. Pradhan, "Adaptive unit protection for lines connecting large solar plants using incremental current ratio," *IEEE Systems Journal*, vol. 16, no. 2, pp. 3272–3283, 2022.

[12] H. J. A. Ferrer(editor) and E. O. SchweitzerIII(editor), *Modern solutions for protection, control, and monitoring of electric power systems*. Pullman, Wash. (2350 NE Hopkins Court, Pullman, WA 99163 USA) Schweitzer Engineering Laboratories, 2010, pp. 79–83.

[13] S. Paladhi and A. K. Pradhan, "Adaptive zone-1 setting following structural and operational changes in power system," *IEEE Trans. Power Del.*, vol. 33, no. 2, pp. 560–569, April 2018.

[14] M. Thompson and A. Somani, "A tutorial on calculating source impedance ratios for determining line length," in *Proc. 68th Annual Conference for Protective Relay Engineers*, March 2015, pp. 833–841.

[15] Siemens, "Distance protection relay for transmission lines," Tech. Rep., 1999, [Online]. Available: ftp://ftp.so-cdu.ru/RZA/Siemens/SIPROTEC%20SA522/7SA522_catalogue.pdf.

[16] Alstom, "Network protection and automation guide," Tech. Rep. 978-0-9568678-0-3, May 2011.

[17] K. E. Arroudi and G. Joos, "Performance of interconnection protection based on distance relaying for wind power distributed generation." *IEEE Trans. Power Del.*, vol. PP, no. 99, pp. 1–1, 2017.

[18] A. K. Pradhan and G. Joos, "Adaptive distance relay setting for lines connecting wind farms," *IEEE Trans. Energy Conv.*, vol. 22, no. 1, pp. 206–213, March 2007.

[19] K. Li, L. Lai, and A. David, "Stand alone intelligent digital distance relay," *IEEE Trans. Power Systems*, vol. 15, no. 1, pp. 137–142, Feb 2000.

[20] J. Upendar, C. Gupta, and G. Singh, "Comprehensive adaptive distance relaying scheme for parallel transmission lines," *IEEE Trans. Power Del.*, vol. 26, no. 2, pp. 1039–1052, April 2011.

[21] A. Banaiemoqadam, A. Hooshyar, and M. A. Azzouz, "A control-based solution for distance protection of lines connected to converter-interfaced sources during asymmetrical faults," *IEEE Trans. Power Del.*, vol. 35, no. 3, pp. 1455–1466, 2020.

[22] Y. Fang, K. Jia, Z. Yang, Y. Li, and T. Bi, "Impact of inverter-interfaced renewable energy generators on distance protection and an improved scheme," *IEEE Trans. Ind. Electr.*, vol. 66, no. 9, pp. 7078–7088, Sep. 2019.

[23] R. W. Kenyon, A. Sajadi, A. Hoke, and B.-M. Hodge, "Open-source PSCAD grid-following and grid-forming inverters and a benchmark for zero-inertia power system simulations," in *IEEE Kansas Power and Energy Conference (KPEC)*, 2021, pp. 1–6.

[24] M. Nagpal, M. Jensen, and M. Higginson, "Protection challenges and practices for interconnecting inverter based resources to utility transmission systems," Working Group C32, Power System Relaying and Control Committee, Tech. Rep., 2020.

[25] Y. Liang, Z. Lu, W. Li, W. Zha, and Y. Huo, "A novel fault impedance calculation method for distance protection against fault resistance," *IEEE Trans. Power Del.*, vol. 35, no. 1, pp. 396–407, 2020.

[26] M. Biswal, B. B. Pati, and A. K. Pradhan, "Directional relaying for double circuit line with series compensation," *IET Gen., Trans., Dist.*, vol. 7, no. 4, pp. 405–413, 2013.

[27] S. Paladhi, A. K. Pradhan, and J. G. Rao, "Accurate superimposed component estimation for improved relay performance during power swing," *IEEE Systems Journal*, vol. 16, no. 4, pp. 6119–6129, 2022.

[28] G. Ziegler, *Numerical Distance Protection: Principles and Applications*. John Wiley & Sons, 2011.

[29] A. Hooshyar, E. F. El-Saadany, and M. Sanaye-Pasand, "Fault type classification in microgrids including photovoltaic DGs," *IEEE Trans. Smart Grid*, vol. 7, no. 5, pp. 2218–2229, Sept 2016.

[30] S. Paladhi, J. R. Kurre, and A. K. Pradhan, "Source-independent zone-1 protection for converter-dominated power networks," *IEEE Transactions on Power Delivery*, vol. 39, no. 1, pp. 341–351, 2024.

[31] PSCAD, "Type 3 wind turbine model," Tech. Rep., November 2018.

[32] PSCAD, "Type 4 wind turbine model," Tech. Rep., December 2018.

[33] C. Sourkounis and P. Tourou, "Grid code requirements for wind power integration in europe," in *Conference Papers in Energy, Hindawi*, 2013, pp. 1–9.

[34] Y. Liang, W. Li, and Y. Huo, "Zone I distance relaying scheme of lines connected to MMC-HVDC stations during asymmetrical faults: Problems, challenges, and solutions," *IEEE Trans. Power Del.*, vol. 36, no. 5, pp. 2929–2941, 2021.

[35] K. Ma, H. K. Høidalen, Z. Chen, and C. L. Bak, "Improved zone 1 top-line tilting scheme for polygonal distance protection in the outgoing line of type-4 wind parks," *CSEE Journal of Power and Energy Systems*, vol. 9, no. 1, pp. 172–184, 2023.

[36] C. Chao, X. Zheng, Y. Weng, Y. Liu, P. Gao, and T. Nengling, "Adaptive distance protection based on the analytical model of additional impedance for inverter-interfaced renewable power plants during asymmetrical faults," *IEEE Trans. Power Del.*, vol. 37, no. 5, pp. 3823–3834, 2022.

[37] V. Makwana and B. Bhalja, "A new digital distance relaying scheme for compensation of high-resistance faults on transmission line," *IEEE Trans. Power Del.*, vol. 27, no. 4, pp. 2133–2140, Oct 2012.

Subhadeep Paladhi (Member, IEEE) received the B.E. degree in Electrical Engineering from University of Burdwan, India, in 2013 and M. Tech. degree in Power Systems from National Institute of Technology Calicut, India in 2015. He received the PhD degree in Electrical Engineering from the Indian Institute of Technology, Kharagpur, India in 2021. From 2021 to 2023, he was with the Department of Electronic and Electrical Engineering, University of Strathclyde, Glasgow, United Kingdom as a research associate. Since 2023, he has been with the Indian Institute of Technology Indore, India as an Assistant Professor in the Department of Electrical Engineering. His current research interests include power system protection and monitoring in the presence of converter-interfaced renewable sources.

Qiteng Hong (Senior Member, IEEE) received the B.Eng. (Hons.) degree and the Ph.D. degree in electronic and electrical engineering from the University of Strathclyde, Glasgow, U.K., in 2011 and 2015, respectively. He is currently a Reader at the University of Strathclyde, Glasgow, U.K. His current research interests include power system protection and control in future networks with high penetration of renewables.

Dr. Hong is a member of the IEEE Working Group P2004 and IEEE Task force on Cloud-Based Control and Co-Simulation of Multi-Party Resources in Energy Internet, and he also was a Regular Member of the completed CIGRE WG B5.50.

Campbell Booth received the B.Eng. and Ph.D. degrees in electrical and electronic engineering from the University of Strathclyde, Glasgow, U.K., in 1991 and 1996, respectively. He is currently a Professor in the Department of Electronic and Electrical Engineering, University of Strathclyde. His research interests include power system protection; plant condition monitoring and intelligent asset management; applications of intelligent system techniques to power system monitoring, protection, and control; knowledge management; and decision support systems.